Research Article

Huiwen Zhang and Dan Jin*

Dynamics in a predator-prey model with predation-driven Allee effect and memory effect

https://doi.org/10.1515/math-2024-0091
received July 31, 2024; accepted October 15, 2024

Abstract: In this article, a diffusive predator-prey model with memory effect and predation-driven Allee effect is considered. Through eigenvalue analysis, the local asymptotic stability of positive constant steady-state solutions is analyzed, and it is found that memory delay affects the stability of positive constant steady-state solutions and induces Hopf bifurcation. The properties of Hopf bifurcating periodic solutions have also been analyzed through the central manifold theorem and the normal form method. Finally, our theoretical analysis results were validated through numerical simulations. It was found that both memory delay and predation-driven Allee effect would cause the positive constant steady-state solution of the model to become unstable, accompanied by the emergence of spatially inhomogeneous periodic solutions. Increasing the memory period will cause periodic oscillations in the spatial distribution of the population. In addition, there would also be high-dimensional bifurcation such as Hopf–Hopf bifurcation, making the spatiotemporal changes of the population more complex.

Keywords: predator-prey, delay, memory effect, Hopf bifurcation

MSC 2020: 34K18, 35B32

1 Introduction

The predator-prey model is one of the important models for studying the interaction between populations, and many scholars have conducted research and obtained many important results [1–3]. The Allee effect is widely present in populations and has been studied by many scholars [4–6]. The Allee effect refers to the fact that when the population density is below a certain threshold, the population may face various challenges such as difficulty in finding mates, decreased group defense capabilities, reduced cooperative predation efficiency, and so on, resulting in a decrease in population growth rate or individual health status. This effect indicates that in some cases, the Allee effect can reflect the relationship between population density and individual survival and reproductive ability, especially when the population size is small, and how the population growth rate is affected by density. There are two common classifications: strong Allee effect and weak Allee effect.

The strong Allee effect refers to the situation where the average individual survival and reproduction rates of a population actually decrease to a level that results in a negative population growth rate, leading to the risk of extinction when the population density is very low. This effect manifests as a threshold (critical population density) on the population growth curve, below which the population tends toward extinction, while above which the population can continue to survive and potentially grow. A typical example of the

* **Corresponding author: Dan Jin,** Department of Mathematics, Northeast Forestry University, Harbin 150040, Heilongjiang, China, e-mail: jindan720@163.com
Huiwen Zhang: Department of Mathematics, Northeast Forestry University, Harbin 150040, Heilongjiang, China

Open Access. © 2024 the author(s), published by De Gruyter. This work is licensed under the Creative Commons Attribution 4.0 International License.

strong Allee effect is the problem of mating. In some species, if the population size is too small, the chance of finding a mate will be greatly reduced, which directly affects the reproductive rate. However, the weak Allee effect refers to the fact that although the population growth rate decreases at low densities, it does not necessarily lead to population extinction. That is to say, when the population density drops to a certain point, the growth rate will slow down, but the population can still be maintained, and when the population size exceeds a certain threshold, the population can resume normal growth. The weak Allee effect may be caused by reduced social interaction, for example, in some animals, individuals may need collective action to defend against predators or search for food.

Recently, the Allee effect driven by the predator has been proposed. Kramer and Drake [7] used an experimental Daphnia-Chaoborus system to illustrate the local extinction of prey caused by the Allee effect driven by predators. In the case of a low population of Daphnia, the Allee effect driven by a higher predation rate accelerates the extinction rate. Wittmer et al. [8] demonstrated the inverse density dependence of large herbivores (reindeer) in their experimental study. In a multi-prey, multipredator ecosystem, the high mortality rate of large herbivores leads to the observations of such inverse density dependency. The main predators of reindeer are believed to be wolves and cougars. Among the 13 forest reindeer subpopulations in British Columbia that feed on tree lichens, 11 subpopulations die primarily due to predation. Sometimes, prey's fear of predators and/or avoidance mechanisms may have a significant impact on predator-prey dynamics rather than direct killing [9,10].

Kayal et al. [11] proposed a predator-prey model with predation-driven Allee effect with the following form:

$$\begin{cases} \dfrac{\mathrm{d}u(t)}{\mathrm{d}t} = ru\left(1 - \dfrac{u}{K}\right)\left(1 - \dfrac{f + \theta v}{f + u}\right) - \dfrac{muv}{a + u}, \\ \dfrac{\mathrm{d}v(t)}{\mathrm{d}t} = sv\left(1 - \dfrac{v}{\alpha + \beta u}\right), \end{cases} \tag{1.1}$$

where the parameters are all positive, and their specific biological significance has been given in [11]. For the completeness of the content, we have listed them in Table 1. The authors [11] mainly analyze the local stability, Hopf bifurcation, and Bogdanov-Tankens bifurcation and obtained that the predator-driven Allee effect may destabilize the model.

In the real world, the spatial distribution of population is inhomogeneous and can lead to diffusion phenomena. Therefore, many scholars have studied predator-prey models with diffusion terms, including self-diffusion and cross diffusion, and have identified new dynamic phenomena such as spatial patterns and spatially inhomogeneous periodic solutions [12,13]. In addition, highly developed animals have a certain degree of memory, and they will spread their predation based on past experience and memory [14,15]. For example, blue whales rely on memory for migration, and animals in polar regions usually determine their spatial movements by judging their footprints. Both wolves and cougars, as predators, possess a certain level of intelligence. They can remember the movement trajectory of reindeer and then spread to the corresponding

Table 1: Biological description of parameters [11]

Parameter	Definition	Parameter	Definition
$u(t)$	Prey density	$v(t)$	Predator density
r	Prey's intrinsic growth rate	K	Prey-carrying capacity
f	Prey-carrying capacity	θ	Allee parameter
m	Encounter rate of predators with prey	a	Half saturation constant
s	Predator's intrinsic growth rate	α	Amount of alternative food
β	Proportionality constant	x	Spatial variable
d_1	Self-diffusion rate of prey	d_2	Self-diffusion rate of predator
d	Memory-based diffusion coefficient	τ	Averaged memory period

positions to capture more reindeer. Many scholars have studied predator-prey models with memory diffusion, often observing stable spatially inhomogeneous periodic solutions, which is different from predator-prey models without memory diffusion that often exhibit stable spatially homogeneous periodic solutions [16–18]. In [16], Wu and Song studied a predator-prey model with distributed memory and maturation delay, including Turing, double Turing, double Hopf, and Turing-Hopf bifurcations, which exhibited richer dynamic properties than models without memory effects. In [17], Jin and Yang mainly studied Hopf bifurcation in a predator-prey model with memory effect and intra-species competition in the predator, which showed the stable inhomogeneous periodic solutions. To our knowledge, almost no work has simultaneously studied predator-driven Allee effects and predator-prey models with memory diffusion. As mentioned above, the relationship between reindeer and wolves (or cougars) is an example of the predator-prey model with both the predator-driven Allee effect and predator memory diffusion, which drives us to study such models.

Inspired by the above, we study the following model with predator-driven Allee effect and memory effect in predator:

$$\begin{cases} \dfrac{\partial u(x,t)}{\partial t} = d_1\Delta u + ru\left(1-\dfrac{u}{K}\right)\left(1-\dfrac{f+\theta v}{f+u}\right) - \dfrac{muv}{a+u}, \\ \dfrac{\partial v(x,t)}{\partial t} = -d\nabla(v\nabla u(t-\tau)) + d_2\Delta v + sv\left(1-\dfrac{v}{\alpha+\beta u}\right), \quad x\in\Omega,\ t>0, \\ \dfrac{\partial u(x,t)}{\partial \bar{v}} = \dfrac{\partial v(x,t)}{\partial \bar{v}} = 0, \quad x\in\partial\Omega,\ t>0, \\ u(x,\theta) = u_0(x,\theta)\geq 0, v(x,\theta) = v_0(x,\theta)\geq 0, \quad x\in\bar{\Omega},\ \theta\in[-\tau,0], \end{cases} \tag{1.2}$$

$-d\nabla(v\nabla u(t-\tau))$ represents the memory effect of predator. The main task of this article is to investigate how the predator-driven Allee effect and memory effect affect the dynamic properties of the model, revealing how they affect the changing trends of the population.

The article structure is as follows. In Section 2, we analyze the local asymptotic stability of positive equilibrium points and the existence of Hopf bifurcation. In Section 3, we provide the normal form of the Hopf bifurcation. In Section 4, we present numerical simulations to validate the theoretical analysis results. In Section 5, we present a conclusion.

2 Stability analysis

$(0,0)$, $(K,0)$, and $(0,\alpha)$ are three boundary equilibrium of model (1.2). If $\beta\theta>1$ and $a<K$, then model (1.2) has unique positive equilibrium (u_*,v_*), where u_* is the positive root of the following equation and $v_*=\alpha+\beta u_*$:

$$\begin{aligned} &\sigma_0u^3+\sigma_1u^2+\sigma_2u+\sigma_3=0, \\ &\sigma_0=r(1-\beta\theta), \quad \sigma_1=-r(K-a)(1-\beta\theta)+\beta Km-a\theta r, \\ &\sigma_2=a\theta r(K-a)-aKr(1-\beta\theta)+Km(\alpha+\beta f), \quad \sigma_3=\alpha K(a\theta r+fm). \end{aligned} \tag{2.1}$$

If $\beta\theta<1$, then model (1.2) may have two positive equilibria.

Denote $E_*(u_*,v_*)$ as a positive equilibrium of (1.2). Linearize system (1.2) at $E_*(u_*,v_*)$

$$\frac{\partial u}{\partial t}\begin{pmatrix}u(x,t)\\u(x,t)\end{pmatrix} = J_1\begin{pmatrix}\Delta u(t)\\\Delta v(t)\end{pmatrix} + J_2\begin{pmatrix}\Delta u(t-\tau)\\\Delta v(t-\tau)\end{pmatrix} + L\begin{pmatrix}u(x,t)\\v(x,t)\end{pmatrix}, \tag{2.2}$$

where

$$J_1=\begin{pmatrix}d_1&0\\0&d_2\end{pmatrix}, \quad J_2=\begin{pmatrix}0&0\\-dv_*&0\end{pmatrix}, \quad L=\begin{pmatrix}a_1&a_2\\s\beta&-s\end{pmatrix},$$

and $a_1 = u_*\left(\frac{mv_*}{(a+u_*)^2} + \frac{r(f(K-2u_*+\theta v_*)+\theta K v_* - u_*^2)}{K(f+u_*)^2}\right)$, $a_2 = -u_*\left(\frac{m}{a+u_*} + \frac{\theta r(1-u_*/K)}{f+u_*}\right) < 0$. The characteristic equation is

$$\lambda^2 + \gamma_n\lambda + \varsigma_n + \chi_n e^{-\lambda\tau} = 0, \quad n \in \mathbb{N}_0, \tag{2.3}$$

where

$$\gamma_n = (d_1+d_2)\mu_n + s - a_1, \quad \varsigma_n = d_1d_2\mu_n^2 - (a_1d_2 - d_1s)\mu_n - s(a_1+a_2\beta), \quad \chi_n = -a_2dv_*\mu_n, \quad \mu_n = \frac{n^2}{l^2}.$$

2.1 Case I: $\tau = 0$

When $\tau = 0$, (2.3) is

$$\lambda^2 + \gamma_n\lambda + \varsigma_n + \chi_n = 0, \quad n = 0, 1, 2, \ldots, \tag{2.4}$$

where $\varsigma_n + \chi_n = d_1d_2\mu_n^2 - \mu_n(a_1d_2 + a_2dv_* - sd_1) - s(a_1 + \beta a_2)$. Make the following hypotheses:

$$(\mathbf{H_1}) \quad s > \max\left\{a_1, \frac{1}{d_1}(a_1d_2 + a_2dv_*)\right\}, \quad a_1 + \beta a_2 < 0,$$

$$(\mathbf{H_2}) \quad s < \frac{1}{d_1}(a_1d_2 + a_2dv_*), a_1 + \beta a_2 < 0, \quad (a_1d_2 + a_2dv_* - sd_1)^2 + 4d_1d_2s(a_1+\beta a_2) < 0,$$

$$(\mathbf{H_3}) \quad s < \frac{1}{d_1}(a_1d_2 + a_2dv_*), a_1 + \beta a_2 < 0, \quad (a_1d_2 + a_2dv_* - sd_1)^2 + 4d_1d_2s(a_1+\beta a_2) > 0.$$

Then, we can obtain the following theorem.

Theorem 2.1. *For system* (1.2) *with* $\tau = 0$, $E_*(u_*, v_*)$ *is locally asymptotically stable under hypothesis* $(\mathbf{H_1})$ *or* $(\mathbf{H_2})$. $E_*(u_*, v_*)$ *may be Turing unstable under hypothesis* $(\mathbf{H_3})$.

Proof. Under hypothesis $(\mathbf{H_1})$ or $(\mathbf{H_2})$, $\gamma_n < 0$ and $\varsigma_n + \chi_n > 0$ for $n = 0, 1, 2, \ldots$, then $E_*(u_*, v_*)$ is locally asymptotically stable. Under hypothesis $(\mathbf{H_3})$, there may be a μ_n such that $\varsigma_n + \chi_n < 0$. This implies equation (2.4) have at least root with positive real parts for the $n \in \mathbb{N}$. However, the roots of equation (2.4) with $n = 0$ have negative real parts. Then, $E_*(u_*, v_*)$ may be Turing unstable. □

2.2 Case II: $\tau > 0$

Assume $(\mathbf{H_1})$ or $(\mathbf{H_2})$ holds. If $\mathrm{i}\omega$ $(\omega > 0)$ is a characteristic root, then

$$-\omega^2 + \gamma_n\mathrm{i}\omega + \varsigma_n + \chi_n(\cos\omega\tau - \mathrm{i}\sin\omega\tau) = 0.$$

So $\cos\omega\tau = \frac{\omega^2 - \varsigma_n}{\chi_n}$, $\sin\omega\tau = \frac{\gamma_n\omega}{\chi_n} > 0$. Then,

$$\omega^4 + (\gamma_n^2 - 2\varsigma_n)\omega^2 + \varsigma_n^2 - \chi_n^2 = 0. \tag{2.5}$$

Denote $p = \omega^2$, then

$$p^2 + (\gamma_n^2 - 2\varsigma_n)p + \varsigma_n^2 - \chi_n^2 = 0, \tag{2.6}$$

$p_n^{\pm} = \frac{1}{2}[-(\gamma_n^2 - 2\varsigma_n) \pm \sqrt{(\gamma_n^2 - 2\varsigma_n)^2 - 4(\varsigma_n^2 - \chi_n^2)}]$. We have

$$\begin{cases} \gamma_n^2 - 2\varsigma_n = (d_1\mu_n - a_1)^2 + (d_2\mu_n + s)^2 + 2a_2\beta s, \\ \varsigma_n - \chi_n = d_1d_2\mu_n^2 - \mu_n(a_1d_2 - d_1s - a_2dv_*) - s(a_1 + a_2\beta), \end{cases}$$

and $\varsigma_n + \chi_n > 0$ under hypothesis ($\mathbf{H_1}$) or ($\mathbf{H_2}$). Obviously, $\lim_{n\to+\infty}(\gamma_n^2 - 2\varsigma_n) = +\infty$ and $\lim_{n\to+\infty}(\varsigma_n - \chi_n) = +\infty$, there are finite numbers of n that make (2.6) have positive roots. Specifically, (2.6) has a unique positive p_n^+ for $n \in \mathbb{M}_1$, two positive roots $p_n^\pm$ for $n \in \mathbb{M}_2$, and no positive root for other nonnegative integer, where $\mathbb{M}_1$ and $\mathbb{M}_2$ are defined as follows:

$$\begin{cases} \mathbb{M}_1 = \{n | \varsigma_n - \chi_n < 0, n \in \mathbb{N}_0\}, \\ \mathbb{M}_2 = \{n | \varsigma_n - \chi_n > 0, \gamma_n^2 - 2\varsigma_n < 0, (\gamma_n^2 - 2\varsigma_n)^2 - 4(\varsigma_n^2 - \chi_n^2) > 0, n \in \mathbb{N}_0\}. \end{cases}$$

Hence, (2.3) has purely imaginary roots $\pm i\omega_n^+$ when $\tau = \tau_n^{j,+}$ and $n \in \mathbb{M}_1$, $\pm i\omega_n^\pm$ when $\tau = \tau_n^{j,\pm}$ and $n \in \mathbb{M}_2$, where

$$\omega_n^\pm = \sqrt{p_n^\pm}, \quad \tau_n^{j,\pm} = \frac{1}{\omega_n^\pm}\arccos\left(\frac{(\omega_n^\pm)^2 - \varsigma_n}{\chi_n}\right) + 2j\pi. \tag{2.7}$$

Lemma 2.1. *If* ($\mathbf{H_1}$) or ($\mathbf{H_2}$) *holds,* $\mathrm{Re}\left(\frac{\mathrm{d}\lambda}{\mathrm{d}\tau}\right)|_{\tau=\tau_n^{j,+}} > 0$, $\mathrm{Re}\left(\frac{\mathrm{d}\lambda}{\mathrm{d}\tau}\right)|_{\tau=\tau_n^{j,-}} < 0$ *for* $\tau_n^{j,\pm} \in \mathbb{S}$ *and* $j = 0, 1, 2, \ldots$.

Proof. From (2.3),

$$\left(\frac{\mathrm{d}\lambda}{\mathrm{d}\tau}\right)^{-1} = \frac{2\lambda + \gamma_n}{\chi_n\lambda e^{-\lambda\tau}} - \frac{\tau}{\lambda}.$$

Then,

$$\begin{aligned} \left[\mathrm{Re}\left(\frac{\mathrm{d}\lambda}{\mathrm{d}\tau}\right)^{-1}\right]_{\tau=\tau_n^{j,\pm}} &= \mathrm{Re}\left[\frac{2\lambda + \gamma_n}{\chi_n\lambda e^{-\lambda\tau}} - \frac{\tau}{\lambda}\right]_{\tau=\tau_n^{j,\pm}} \\ &= \left[\frac{1}{\gamma_n^2\omega^2 + (\varsigma_n - \omega)^2}(2\omega^2 + \gamma_n^2 - 2\varsigma_n)\right]_{\tau=\tau_n^{j,\pm}} \\ &= \pm\left[\frac{1}{\gamma_n^2\omega^2 + (\varsigma_n - \omega)^2}\sqrt{(\gamma_n^2 - 2\varsigma_n)^2 - 4(\varsigma_n^2 - \chi_n^2)}\right]_{\tau=\tau_n^{j,\pm}}. \end{aligned}$$

Therefore, $\mathrm{Re}\left(\frac{\mathrm{d}\lambda}{\mathrm{d}\tau}\right)\Big|_{\tau=\tau_n^{j,+}} > 0$, $\mathrm{Re}\left(\frac{\mathrm{d}\lambda}{\mathrm{d}\tau}\right)\Big|_{\tau=\tau_n^{j,-}} < 0$. □

Denote $\tau_* = \min\{\tau_n^{0,\pm} | n \in \mathbb{M}_{1,2}\}$.

Theorem 2.2. *Suppose* ($\mathbf{H_1}$) or ($\mathbf{H_2}$) *holds.*

- *For all* $\tau > 0$, $E_*(u_*, v_*)$ *is stable if* $\mathbb{S} = \varnothing$.
- *For* $\tau \in [0, \tau_*)$, $E_*(u_*, v_*)$ *is stable if* $\mathbb{S} \neq \varnothing$. *For* $\tau \in (\tau_*, \tau_* + \varepsilon)$ (*some* $\varepsilon > 0$), $E_*(u_*, v_*)$ *is unstable if* $\mathbb{S} \neq \varnothing$.
- *For* $\tau = \tau_n^{j,+}$ ($\tau = \tau_n^{j,-}$), $j = 0, 1, 2, \ldots$, $\tau_n^{j,\pm} \in \mathbb{S}$, *Hopf bifurcation occurs at* (u_*, v_*).

3 Property of Hopf bifurcation

The normal form is

$$\dot{z} = Bz + \frac{1}{2}\begin{pmatrix} B_1 z_1 \varepsilon \\ \bar{B}_1 z_2 \varepsilon \end{pmatrix} + \frac{1}{3!}\begin{pmatrix} B_2 z_1^2 z_2 \varepsilon \\ \bar{B}_2 z_1 z_2^2 \varepsilon \end{pmatrix} + O(|z|\varepsilon^2 + |z^4|), \tag{3.1}$$

where

$$B_1 = 2i\tilde{\omega}\psi^T\phi, \quad B_2 = B_{21} + \frac{3}{2}(B_{22} + B_{23}).$$

By coordinate transformation $z_1 = \omega_1 - i\omega_2$, $z_2 = \omega_1 + i\omega_2$, and $\omega_1 = \rho\cos\xi$, $\omega_2 = \rho\sin\xi$, the normal form (3.1) can be rewritten as

$$\dot{\rho} = K_1\varepsilon\rho + K_2\rho^3 + O(\rho\varepsilon^2 + |(\rho, \varepsilon)|^4), \tag{3.2}$$

where $K_1 = \frac{1}{2}\mathrm{Re}(B_1)$, $K_2 = \frac{1}{3!}\mathrm{Re}(B_2)$. The detailed computation is given in Appendix A by the work [19].

Theorem 3.1. *The Hopf bifurcation is forward (backward) when* $K_1K_2 < 0$ (> 0), *and the bifurcating periodic orbits is stable (unstable) for* $K_2 < 0$ (> 0).

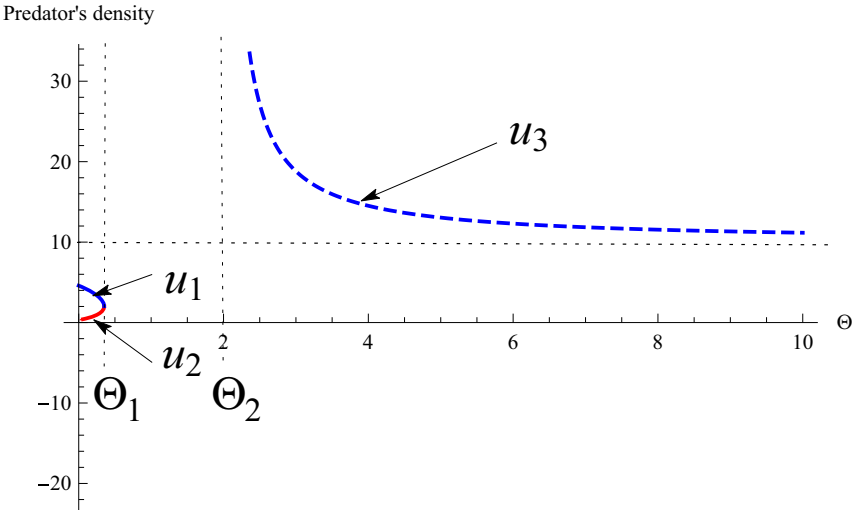

Figure 1: The predator's density with parameter θ, where $\theta_1 \approx 0.3512$ and $\theta_2 = 2$.

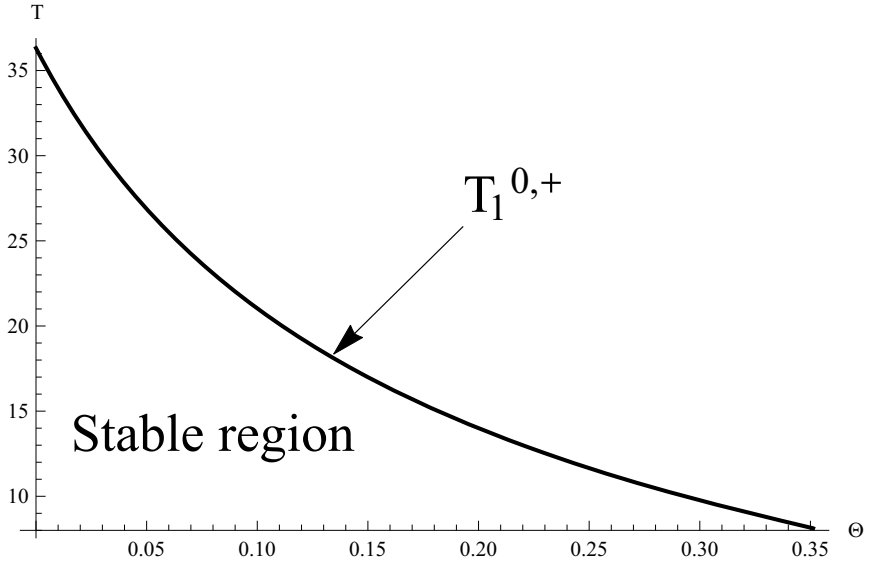

Figure 2: Bifurcation diagram with θ.

4 Numerical simulations

In this section, some numerical simulations are performed by the Matlab. Choose the parameters

$$r = 0.5, \quad K = 10, \quad f = 0.2, \quad m = 0.5, \quad a = 0.8, \quad \alpha = 0.5, \quad \beta = 0.5, \quad s = 0.2. \tag{4.1}$$

To numerically solve equation (1.2), taking the time step Δt as $\tau/500$ and space step Δx as $2\pi/50$, the finite difference scheme is used to replace approximately the Laplacian operator, and the Euler difference scheme is used to replace approximately the partial derivative regarding time.

We give the existence of positive equilibrium (predator's density) with θ in Figure 1. When $\theta \in (0, \theta_1)$, model (1.2) has two positive equilibria (u_1, v_1) and (u_2, v_2) (always unstable), and two positive equilibria will degenerate into one when $\theta = \theta_1$. When $\theta \in (\theta_1, \theta_2)$, model (1.2) has no positive equilibrium. However, when $\theta > \theta_2$, model (1.2) always has a unique positive equilibrium which is unstable under parameters (4.1). This means that the Allee parameter θ has an impact on the existence and stability of constant steady-state solutions.

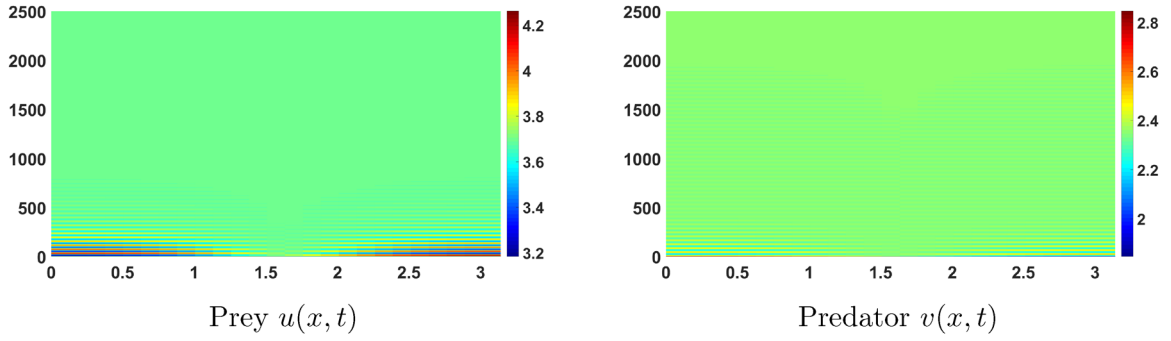

Figure 3: Numerical simulations of model (1.2) with $\tau = 12$. The positive constant steady-state solution (u_1, v_1) is locally asymptotically stable, meaning that densities of predators and preys are evenly distributed in space and gradually tends to a positive equilibrium point (u_1, v_1).

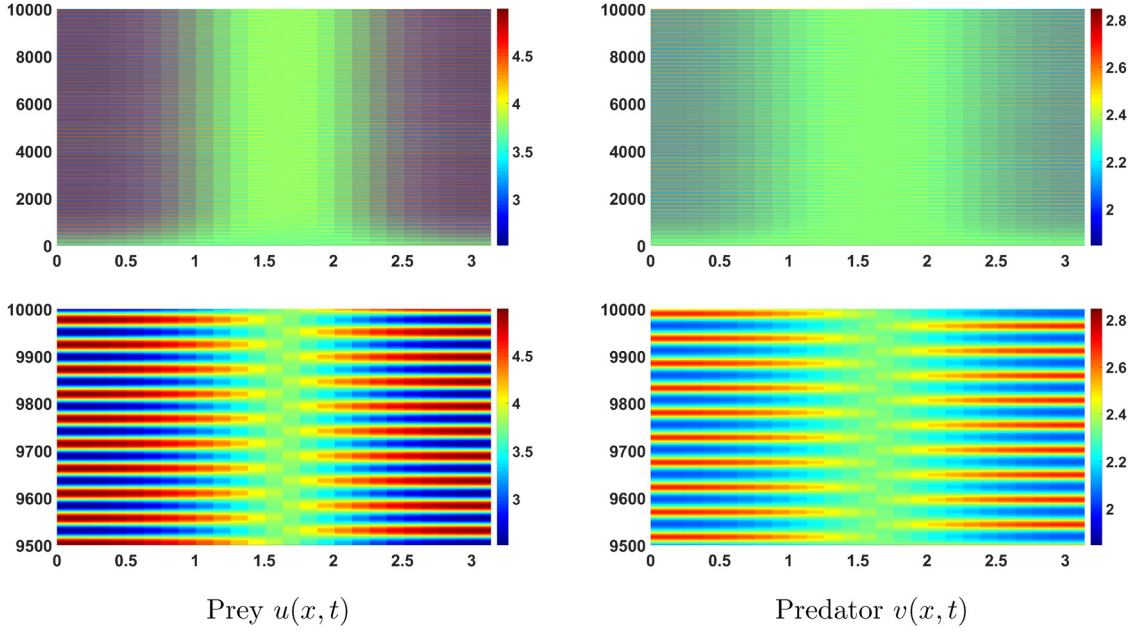

Figure 4: Numerical simulations of model (1.2) with $\tau = 18$. The inhomogeneous periodic solution is stable, meaning that densities of predators and preys are unevenly distributed in space and oscillates within a certain period.

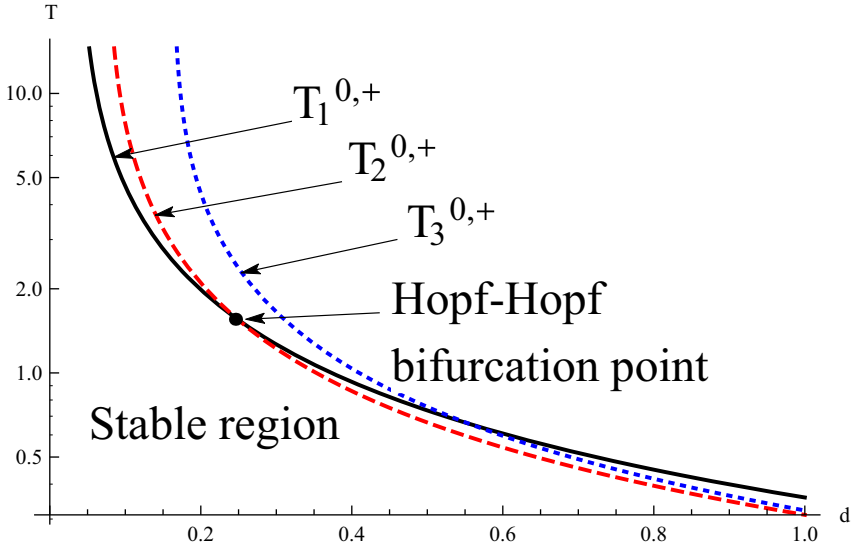

Figure 5: Bifurcation diagram with d.

If we choose $d_1 = 0.1$, $d_2 = 0.2$, $d = 0.05$, and $l = 1$, the bifurcation diagram is shown in Figure 2. We can see that memory delay can cause the original system to become unstable and accompanied by the emergence of spatially inhomogeneous periodic solutions. As the Allee parameter θ increases, the stable region of the positive constant steady-state solution becomes smaller.

If we choose $d_1 = 0.1$, $d_2 = 0.2$, $d = 0.05$, $l = 1$, and $\theta = 0.2$, then $(u_1, v_1) \approx (3.6932, 2.3466)$ and $(\mathbf{H_1})$ holds, $\mathbb{M}_1 = \{1\}, \mathbb{M} = \varnothing, \tau_* = \tau_1^{0,+} \approx 16.3302$ and $K_1 \approx 0.0108 > 0, K_2 \approx -0.0046 < 0$. When the hysteresis is less than the critical value τ_*, the positive constant steady-state solution is stable (Figure 3). When the hysteresis is greater than the critical value τ_*, a stable inhomogeneous periodic solution of mode-1 appears (Figure 4).

If we choose $d_1 = 0.1$, $d_2 = 0.2$, $l = 1$, and $\theta = 0.2$, the bifurcation diagram with parameter d is shown in Figure 5. As d increases, the stable region of the positive constant steady-state solution becomes smaller. The system may also exhibit a Hopf–Hopf bifurcation, which is a codimension 2 bifurcation, making the existence of the population more complex. This means that memory-based diffusion coefficient d will change the stability of the steady-state solution and induce bifurcation periodic solutions, causing periodic oscillations in the density of prey and predator over time.

If we choose $d_1 = 0.1$, $d_2 = 0.2$, $d = 0.4$, $l = 1$, and $\theta = 0.2$, then $(u_1, v_1) \approx (3.6932, 2.3466)$ and $(\mathbf{H_1})$ holds, $\mathbb{M}_1 = \{1, 2, 3\}, \mathbb{M} = \varnothing, \tau_* = \tau_2^{0,+} \approx 0.8607$ and $K_1 \approx 0.0126 > 0, K_2 \approx -0.1451 < 0$. When the hysteresis is less than

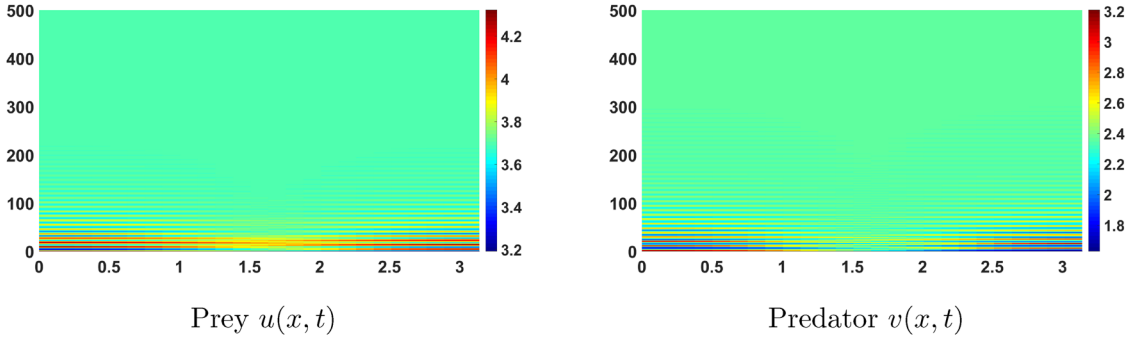

Figure 6: Numerical simulations of model (1.2) with $\tau = 0.8$. The positive constant steady-state solution (u_1, v_1) is locally asymptotically stable, meaning that densities of predators and preys are evenly distributed in space and gradually tends to a positive equilibrium point (u_1, v_1).

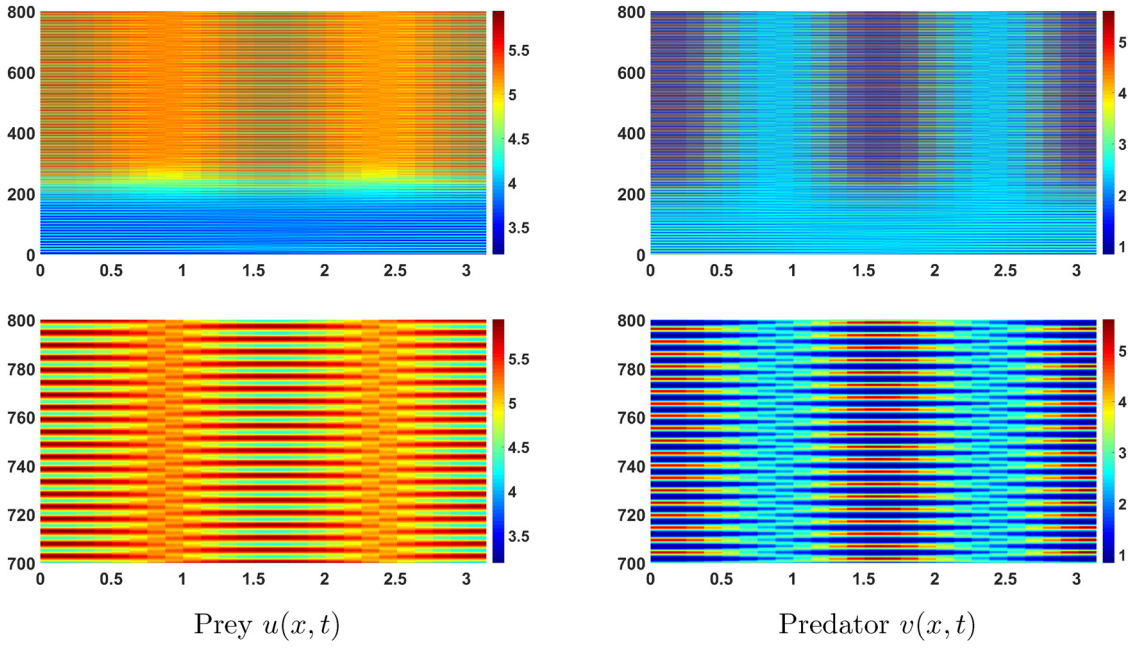

Figure 7: Numerical simulations of model (1.2) with $\tau = 0.88$. The inhomogeneous periodic solution is stable, meaning that densities of predators and preys are unevenly distributed in space and oscillates within a certain period.

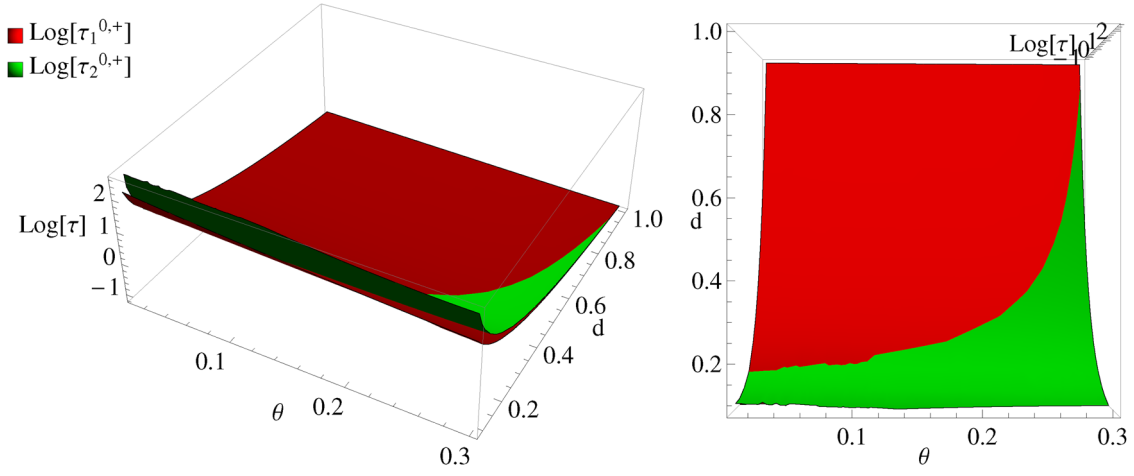

Figure 8: Bifurcation diagram with θ and d.

the critical value τ_*, the positive constant steady-state solution is stable (Figure 6). When the hysteresis is greater than the critical value τ_*, a stable inhomogeneous periodic solution of mode-2 appears (Figure 7).

If we choose $d_1 = 0.1$, $d_2 = 0.2$, and $l = 1$, the bifurcation diagram with θd is shown in Figure 8. It can be seen that the system dynamics is altered with both memory and predator-driven Allee effects. We can see from the left side of Figure 8 that the stable region of the constant steady-state solution decreases continuously with the increase of parameters, accompanied by the occurrence of periodic oscillations. The specific occurrence of inhomogeneous periodic solutions with mode-1 or mode-2 depends on the interval in which the parameters are located (right side of Figure 8).

5 Conclusion

In this article, we study a predator-prey model with memory effect and predation-driven Allee effect. Using memory delay τ as a parameter, we mainly analyzed the local asymptotic stability of the positive constant steady-state solution of the model and the existence of Hopf bifurcation. We also analyzed the properties of bifurcating periodic solutions using the central manifold theorem, and the normal form method.

Memory delay affects the stability of constant steady-state solutions. With the increase of time delay, the stability of constant steady-state solutions will be destroyed, accompanied by the emergence of periodic solutions, that is, Hopf bifurcation. Biologically speaking, memory delay affects the spatial distribution of prey and predator density, and exhibits periodic oscillations. In addition, an increase in the Allee parameter θ will be detrimental to the stability of constant steady-state solutions, leading to spatially inhomogeneous oscillations in population density. Similarly, an increase in memory diffusion coefficient d is not conducive to a uniform distribution of population density and can lead to high-dimensional Hopf–Hopf bifurcation, making the spatiotemporal distribution of prey and predators more complex.

Acknowledgement: The authors are grateful for the reviewer's valuable comments that improved the manuscript.

Funding information: This research was supported by the Fundamental Research Funds for the Central Universities (Grant No. 2572022BC01), and College Students Innovations Special Project funded by Northeast Forestry University.

Author contributions: All authors have accepted responsibility for the entire content of this manuscript and consented to its submission to the journal, reviewed all the results and approved the final version of the manuscript. DJ designed the experiments and HZ carried them out. All authors read and approved the final manuscript.

Conflict of interest: The authors state no conflict of interest.

References

[1] Y. Ma and R. Yang, *Hopf-Hopf bifurcation in a predator-prey model with nonlocal competition and refuge in prey*, Discrete Contin. Dyn. Syst. Ser. B **29** (2024), no. 6, 2582–2609, DOI: https://doi.org/10.3934/dcdsb.2023193.

[2] R. Han, L. N. Guin, and S. Acharya, *Complex dynamics in a reaction-cross-diffusion model with refuge depending on predator-prey encounters*, Eur. Phys. J. Plus **137** (2022), no. 1, 134, DOI: https://doi.org/10.1140/epjp/s13360-022-02358-7.

[3] F. Wang and R. Yang, *Spatial pattern formation driven by the cross-diffusion in a predator-prey model with Holling type functional response*, Chaos Solitons Fractals **174** (2022), 113890, DOI: https://doi.org/10.1016/j.chaos.2023.113890.

[4] F. Wang and R. Yang, *Dynamics of a delayed reaction-diffusion predator-prey model with nonlocal competition and double Allee effect in prey* ł143, Int. J. Biomath. **2024** (2024), 2350097, DOI: https://doi.org/10.1142/S1793524523500973.

[5] G. Mandal, L. N. Guin, S. Chakravarty, A. Rojas-Palma, and E. Gonzalez-Olivares, *Allee-induced bubbling phenomena in an interacting species model*, Chaos Solitons Fractals **184** (2024), 114949, DOI: https://doi.org/10.1016/j.chaos.2024.114949.

[6] F. Wang, R. Yang, and X. Zhang, *Turing patterns in a predator-prey model with double Allee effect*, Math. Comput. Simulation **220** (2024), 170–191, DOI: https://doi.org/10.1016/j.matcom.2024.01.015.

[7] A. M. Kramer and J. M. Drake, *Experimental demonstration of population extinction due to a predator-driven Allee effect*, J. Anim. Ecol. **79** (2010), no. 3, 633–639, DOI: https://doi.org/10.1111/j.1365-2656.2009.01657.x.

[8] H. U. Wittmer, A. R. Sinclai, and B. N McLellan, *The role of predation in the decline and extirpation of woodland caribou*, Oecologia **144** (2005), no. 2, 257–267, DOI: https://doi.org/10.1007/s00442-005-0055-y.

[9] S. Pal, S. Majhi, S. Mandal, and N. Pal, *Role of fear in a predator-prey model with Beddington-DeAngelis functional response*, Z. Naturforsch. A Phys. Sci.. **74** (2019), no. 7, 581–595, DOI: https://doi.org/10.1515/zna-2018-0449.

[10] S. Pal, N. Pal, S. Samanta, and J. Chattopadhyay, *Effect of hunting cooperation and fear in a predator-prey model*, Ecol. Complex. **39** (2019), 100770, DOI: https://doi.org/10.1016/j.ecocom.2019.100770.

[11] K. Kayal, S. Samanta, and J. Chattopadhyay, *Impacts of predation-driven Allee effect in a predator-prey model*, Internat. J. Bifur. Chaos Appl. Sci. Engrg. **33** (2023), no. 2, 2350023, DOI: https://doi.org/10.1142/S0218127423500232.
[12] Y. Sun and S. Chen, *Stability and bifurcation in a reaction-diffusion-advection predator-prey model*, Calc. Var. Partial Differential Equations **62** (2023), no. 2, 1–31, DOI: https://doi.org/10.1007/s00526-022-02405-2.
[13] G. Mandal, S. Dutta, and G. S. Chakravarty, *Spatiotemporal behavior of a generalist predator-prey system with harvesting phenomena*, Math. Methods Appl. Sci. **47** (2024), no. 4, 2827–2867, DOI: https://doi.org/10.1002/mma.9780.
[14] J. Shi, C. Wang, H. Wang, and Y. P. Yan, *Diffusive spatial movement with memory*, J. Dynam. Differential Equations **32** (2020), no. 2, 979–1002, DOI: https://doi.org/10.1007/s10884-019-09757-y.
[15] J. Shi, C. Wang, and H. Wang, *Diffusive spatial movement with memory and maturation delays*, Nonlinearity **32** (2019), no. 9, 3188–3208, DOI: https://doi.org/10.1088/1361-6544/ab1f2f.
[16] S. Wu and Y. Song, *Spatial movement with distributed memory and maturation delay*, Qual. Theory Dyn. Syst. **23** (2024), no. 3, 117, DOI: https://doi.org/10.1007/s12346-024-00975-4.
[17] D. Jin and R. Yang, *Hopf bifurcation in a predator-prey model with memory effect and intra-species competition in predator*, J. Appl. Anal. Comput. **13** (2023), no. 3, 1321–1335, DOI: https://doi.org/10.11948/20220127.
[18] Q. Shi, J. Shi, and H. Wang, *Spatial movement with distributed delay*, J. Math. Biol. **82** (2021), 33, DOI: https://doi.org/10.1007/s00285-021-01588-0.
[19] Y. Song, Y. Peng, and T. Zhang, *The spatially inhomogeneous Hopf bifurcation induced by memory delay in a memory-based diffusion system*, J. Differential Equations **300** (2021), no. 5, 597–624, DOI: https://doi.org/10.1016/j.jde.2021.08.010.

Appendix

A Computation of normal form

Similar to [19], denote the critical value as $\tilde{\tau}$ and eigenvalue as $\pm i\omega_n$. Move the steady-state solution to the origin.

$$\begin{cases} \dfrac{\partial u}{\partial t} = \tau\left[d_1\Delta u + r(u+u_*)\left(1-\dfrac{u+u_*}{K}\right)\left(1-\dfrac{f+\theta(v+v_*)}{f+u+u_*}\right) - \dfrac{m(u+u_*)(v+v_*)}{a+u+u_*}\right] \\ \dfrac{\partial v}{\partial t} = \tau\left[-d\nabla((v+v_*)\nabla(u(t-1)+u_*)) + d_2\Delta v + s(v+v_*)\left(1-\dfrac{v+v_*}{a+\beta(u+u_*)}\right)\right]. \end{cases} \tag{A1}$$

Define $\mathbb{X} = \left\{U=(u,v)^T \in W^{2,2}(0,l\pi)^2, (\frac{\partial u}{\partial x}, \frac{\partial v}{\partial x})|_{x=0,l\pi} = 0\right\}$, with

$$[Y_1, Y_2] = \int_0^{l\pi} Y_1^T Y_2 \mathrm{d}x, \quad \text{for } Y_1, Y_2 \in \mathbb{X},$$

and $\mathbb{C} = C([-1,0];\mathbb{X})$. Denote ε is small perturbation, then $\tau = \tilde{\tau} + \varepsilon$. System (A1) is

$$\frac{\mathrm{d}U(t)}{\mathrm{d}t} = d(\varepsilon)\Delta(U_t) + L(\varepsilon)(U_t) + F(U_t,\varepsilon), \tag{A2}$$

where $d(\varepsilon)\Delta(\varphi) = d_0\Delta(\varphi) + F^d(\varphi,\varepsilon)$, $L(\varepsilon)(\varphi) = (\tilde{\tau}+\varepsilon)A\varphi(0)$,

$$F(\varphi,\varepsilon) = (\tilde{\tau}+\varepsilon)\begin{pmatrix} h(\phi^{(1)}(0)+u_*, \phi^{(2)}(0)+v_*) \\ g(\phi^{(1)}(0)+u_*, \phi^{(2)}(0)+v_*) \end{pmatrix} - L(\varepsilon)(\varphi)$$

and

$$d_0\Delta(\varphi) = \tilde{\tau}J_1\varphi_{xx}(0) + \tilde{\tau}J_2\varphi_{xx}(-1),$$

$$F^d(\varphi,\varepsilon) = -d(\tilde{\tau}+\varepsilon)\begin{pmatrix} 0 \\ \phi_x^{(1)}(-1)\phi_x^{(2)}(0) + \phi_{xx}^{(1)}(-1)\phi^{(2)}(0) \end{pmatrix} + \varepsilon\begin{pmatrix} d_1\phi_{xx}^{(1)}(0) \\ -dv_*\phi_{xx}^{(1)}(-1) + d_2\phi_{xx}^{(2)}(0) \end{pmatrix}.$$

Denote $L_0(\varphi) = \tilde{\tau}A\varphi(0)$,

$$\frac{\mathrm{d}U(t)}{\mathrm{d}t} = d_0\Delta(U_t) + L_0(U_t) + \tilde{F}(U_t,\varepsilon), \tag{A3}$$

where $\tilde{F}(\varphi,\varepsilon) = \varepsilon A\varphi(0) + F(\varphi,\varepsilon) + F^d(\varphi,\varepsilon)$. The characteristic equation is $\tilde{I}_n(\lambda) = det(\tilde{M}_n((\lambda))) = 0$, where

$$\tilde{M}_n(\lambda) = \lambda I_2 + \tilde{\tau}\mu_n D_1 + \tilde{\tau}e^{-\lambda}\mu_n D_2 - \tilde{\tau}A. \tag{A4}$$

Denote normalized eigenfunctions

$$z_n(x) = \frac{\cos\frac{nx}{l}}{||\cos\frac{nx}{l}||_{2,2}} = \begin{cases} \dfrac{1}{l\pi} & n=0, \\ \dfrac{\sqrt{2}}{l\pi}\cos\dfrac{nx}{l} & n\neq 0. \end{cases} \tag{A5}$$

Set $\beta_n^{(j)} = z_n(x)e_j$, $j=1,2$, where $e_1=(1,0)^T$ and $e_2=(0,1)^T$. Define $\eta_n(\theta) \in BV([-1,0],\mathbb{R}^2)$, such that

$$\int_{-1}^{0} \mathrm{d}\eta^n(\theta)\phi(\theta) = L_0^d(\varphi(\theta)) + L_0(\varphi(\theta)), \varphi \in C,$$

$C = C([-1, 0], \mathbb{R}^2)$, $C^* = C([0, 1], \mathbb{R}^{2*})$, and

$$\langle \psi(s), \varphi(\theta) \rangle = \psi(0)\varphi(0) - \int_{-1}^{0}\int_{0}^{\theta} \psi(\xi - \theta) d\eta^n(\theta)\varphi(\xi)d\xi, \ \psi \in C^*, \varphi \in C. \tag{A6}$$

Let $\wedge = \{i\tilde{\omega}, -i\tilde{\omega}\}$, the eigenspace P, and corresponding adjoint space P^*. Decompose $C = P \oplus Q$, where $Q = \{\varphi \in C : \langle \psi, \varphi \rangle = 0, \forall \psi \in P^*\}$. Choose $\Phi(\theta) = (\phi(\theta), \bar{\phi}(\theta))$, $\Psi(\theta) = col(\psi^T(s), \bar{\psi}^T(s))$, where

$$\phi(\theta) = \phi e^{i\tilde{\omega}\theta} = \begin{pmatrix} \phi_1(\theta) \\ \phi_2(\theta) \end{pmatrix}, \quad \psi(s) = \psi e^{-i\tilde{\omega}s} = \begin{pmatrix} \psi_1(s) \\ \psi_2(s) \end{pmatrix},$$
$$\phi = \begin{pmatrix} 1 \\ (d_1\mu_n i\tilde{\omega} - a_1)/a_2 \end{pmatrix}, \quad \psi = M\begin{pmatrix} 1 \\ a_2/(d_2\mu_n + i\tilde{\omega} + s) \end{pmatrix},$$

and

$$M = \left(-\frac{a_1 - a_2 \mathrm{d}\tau v_* \mu_n e^{-i\tilde{\omega}} e^{-i\tilde{\omega}\tilde{\tau}} - d_1\mu_n - d_2\mu_n - s - 2i\tilde{\omega}}{d_2\mu_n + s + i\tilde{\omega}} \right)^{-1}.$$

Denote

$$f_{20} = \begin{pmatrix} f_{20}^{(1)} \\ f_{20}^{(2)} \end{pmatrix}, \quad f_{11} = \begin{pmatrix} f_{11}^{(1)} \\ f_{11}^{(2)} \end{pmatrix}, \quad f_{02} = \begin{pmatrix} f_{02}^{(1)} \\ f_{02}^{(2)} \end{pmatrix},$$
$$f_{30} = \begin{pmatrix} f_{30}^{(1)} \\ f_{30}^{(2)} \end{pmatrix}, \quad f_{21} = \begin{pmatrix} f_{21}^{(1)} \\ f_{21}^{(2)} \end{pmatrix}, \quad f_{12} = \begin{pmatrix} f_{12}^{(1)} \\ f_{12}^{(2)} \end{pmatrix}, \quad f_{03} = \begin{pmatrix} f_{03}^{(1)} \\ f_{03}^{(2)} \end{pmatrix},$$

where

$$\begin{cases} f_{20}^{(1)} = \dfrac{fr(f(K - 3u_* + \theta v_*) + \theta K v_* - 3u_*^2)}{K(f + u_*)^3}, f_{11}^{(1)} = \dfrac{\theta r(-fK + 2fu_* + u_*^2)}{K(f + u_*)^2} - \dfrac{am}{(a + u_*)^2}, \\ f_{02}^{(1)} = 0, f_{30}^{(1)} = 6\left(v_*\left(-\dfrac{am}{(a + u_*)^4} - \dfrac{f\theta r(f + K)}{K(f + u_*)^4} \right) - \dfrac{f^2 r(f + K)}{K(f + u_*)^4} \right), \\ f_{21}^{(1)} = \dfrac{2am}{(a + u_*)^3} + \dfrac{2f\theta r(f + K)}{K(f + u_*)^3}, f_{12}^{(1)} = 0, f_{03}^{(1)} = 0, f_{20}^{(2)} = -\dfrac{2\beta^2 s}{\alpha + \beta u_*}, f_{11}^{(2)} = \dfrac{2\beta s}{\alpha + \beta u_*}, \\ f_{02}^{(2)} = -\dfrac{2s}{\alpha + \beta u_*}, f_{30}^{(2)} = \dfrac{6v_*(1 + bv_*)(a + cv_*)^2\beta}{(1 + au_* + bv_* + cu_*v_*)^4}, f_{03}^{(2)} = \dfrac{6\beta^3 s}{(\alpha + \beta u_*)^2}, \\ f_{21}^{(2)} = -\dfrac{4\beta^2 s}{(\alpha + \beta u_*)^2}, f_{12}^{(2)} = \dfrac{2\beta s}{(\alpha + \beta u_*)^2}, f_{03}^{(2)} = 0. \end{cases}$$

Compute the following parameters:

$$\begin{aligned} A_{20} &= f_{20}\phi_1(0)^2 + f_{02}\phi_2(0)^2 + 2f_{11}\phi_1(0)\phi_2(0) = \overline{A}_0 2, \\ A_{11} &= 2f_{20}\phi_1(0)\bar{\phi}_1(0) + 2f_{02}\phi_2(0)\bar{\phi}_2(0) + 2f_{11}(\phi_1(0)\bar{\phi}_2(0) + \bar{\phi}_1(0)\phi_2(0)), \\ A_{21} &= 3f_{30}\phi_1(0)^2\bar{\phi}_1(0) + 3f_{03}\phi_2(0)^2\bar{\phi}_2(0) + 3f_{21}(\phi_1(0)^2\bar{\phi}_2(0) + 2\phi_1(0)\bar{\phi}_1(0)\phi_2(0)) \\ &\quad + 3f_{12}(\phi_2(0)^2\bar{\phi}_1(0) + 2\phi_2(0)\bar{\phi}_2(0)\phi_1(0)), \end{aligned} \tag{A7}$$

$$A_{20}^d = -2\mathrm{d}\tau\begin{pmatrix} 0 \\ \phi_1(0)(-1)\phi_2(0)(0) \end{pmatrix} = \bar{A}_{02}^d, A_{11}^d = -2\mathrm{d}\tau\begin{pmatrix} 0 \\ 2\mathrm{Re}[\phi_1(-1)\bar{\phi}_2(0)] \end{pmatrix},$$

and $\widetilde{A}_{j_1 j_2} = A_{j_1 j_2} - 2\mu_n A_{j_1 j_2}^d$ for $j_1, j_2 = 0, 1, 2, j_1 + j_2 = 2$. In addition, $h_{0,20}(\theta) = \frac{1}{l\pi}(\widetilde{M}_0(2i\tilde{\omega}))^{-1}A_{20}e^{2i\tilde{\omega}\theta}$, $h_{0,11}(\theta) = \frac{1}{l\pi}(\widetilde{M}_0(0))^{-1}A_{11}$, $h_{2n,20}(\theta) = \frac{1}{2l\pi}(\widetilde{M}_{2n}(2i\tilde{\omega}))^{-1}\widetilde{A}_{20}e^{2i\tilde{\omega}\theta}$, $h_{2n,11}(\theta) = \frac{1}{l\pi}(\widetilde{M}_{2n}(0))^{-1}\widetilde{A}_{11}$.

$$S_2(\phi(\theta), h_{n,q_1q_2}(\theta)) = 2\phi_1 h^{(1)}_{n,q_1q_2} f_{20} + 2\phi_2 h^{(2)}_{n,q_1q_2} f_{02} + 2(\phi_1 h^{(2)}_{n,q_1q_2} + \phi_2 h^{(1)}_{n,q_1q_2}) f_{11},$$

$$S_2(\bar{\phi}(\theta), h_{n,q_1q_2}(\theta)) = 2\bar{\phi}_1 h^{(1)}_{n,q_1q_2} f_{20} + 2\bar{\phi}_2 h^{(2)}_{n,q_1q_2} f_{02} + 2(\bar{\phi}_1 h^{(2)}_{n,q_1q_2} + \bar{\phi}_2 h^{(1)}_{n,q_1q_2}) f_{11},$$

$$S_2^{d,1}(\phi(\theta), h_{0,11}(\theta)) = -2d\tilde{\tau}\begin{pmatrix} 0 \\ \phi_1(-1)h^{(2)}_{0,11}(0) \end{pmatrix},\ S_2^{d,1}(\bar{\phi}(\theta), h_{0,11}(\theta)) = -2d\tilde{\tau}\begin{pmatrix} 0 \\ \bar{\phi}_1(-1)h^{(2)}_{0,20}(0) \end{pmatrix},$$

$$S_2^{d,1}(\phi(\theta), h_{2n,11}(\theta)) = -2d\tilde{\tau}\begin{pmatrix} 0 \\ \phi_1(-1)h^{(2)}_{2n,11}(0) \end{pmatrix},\ S_2^{d,1}(\bar{\phi}(\theta), h_{2n,20}(\theta)) = -2d\tilde{\tau}\begin{pmatrix} 0 \\ \bar{\phi}_1(-1)h^{(2)}_{2n,20}(0) \end{pmatrix},$$

$$S_2^{d,2}(\phi(\theta), h_{2n,11}(\theta)) = -2d\tilde{\tau}\begin{pmatrix} 0 \\ \phi_1(-1)h^{(2)}_{2n,11}(0) \end{pmatrix} - 2d\tilde{\tau}\begin{pmatrix} 0 \\ \phi_2(0)h^{(1)}_{2n,11}(-1) \end{pmatrix},$$

$$S_2^{d,2}(\bar{\phi}(\theta), h_{2n,20}(\theta)) = -2d\tilde{\tau}\begin{pmatrix} 0 \\ \bar{\phi}_1(-1)h^{(2)}_{2n,20}(0) \end{pmatrix} - 2d\tilde{\tau}\begin{pmatrix} 0 \\ \bar{\phi}_2(0)h^{(1)}_{2n,20}(-1) \end{pmatrix},$$

$$S_2^{d,3}(\phi(\theta), h_{2n,11}(\theta)) = -2d\tilde{\tau}\begin{pmatrix} 0 \\ \phi_2(0)h^{(1)}_{2n,11}(-1) \end{pmatrix},\ S_2^{d,3}(\bar{\phi}(\theta), h_{2n,20}(\theta)) = -2d\tilde{\tau}\begin{pmatrix} 0 \\ \bar{\phi}_1(0)h^{(2)}_{2n,20}(-1) \end{pmatrix}.$$

Then

$$B_{21} = \frac{3}{2l\pi}\psi^T A21,$$

$$B_{22} = \frac{1}{l\pi}\psi^T(S_2(\phi(\theta), h_{0,11}(\theta)) + S_2(\bar{\phi}(\theta), h_{0,20}(\theta))) + \frac{1}{2l\pi}\psi^T(S_2(\phi(\theta), h_{2n,11}(\theta)) + S_2(\bar{\phi}(\theta), h_{2n,20}(\theta))),$$

$$B_{23} = -\frac{1}{l\pi}\mu_n\psi^T(S_2^{d,1}(\phi(\theta), h_{0,11}(\theta)) + S_2^{d,1}(\bar{\phi}(\theta), h_{0,20}(\theta))) + \frac{1}{2l\pi}\psi^T\sum\nolimits_{j=1,2,3} b^{(j)}_{2n}(S_2^{d,j}(\phi(\theta), h_{2n,11}(\theta)) + S_2^{d,j}(\bar{\phi}(\theta), h_{2n,20}(\theta))),$$

where $b^{(1)}_{2n} = -\mu_n$, $b^{(2)}_{2n} = -2\mu_n$, $b^{(3)}_{2n} = -4\mu_n$.